CHARACTERIZED FAULT MODEL FOR PREDICTION OF GROUND MOTIONS INCLUDING FLING STEP IN THE NEAR-FAULT REGION

S. Tanaka [1], J. Kaneda [2], K. Hikima [3], Y. Hisada [4]

[1] *Tokyo Electric Power Services Co., Ltd., M. Engineering, s.tanaka@tepsco.co.jp*
[2] *Tokyo Electric Power Services Co., Ltd., M. Engineering, junpei-kaneda@tepsco.co.jp*
[3] *Specialist, Tokyo Electric Power Company, Dr. Science, hikima.kazuhito@tepco.co.jp*
[4] *Professor, School of Architecture, Kogakuin University, Dr. Engineering, hisada@cc.kogakuin.ac.jp*

Abstract

We propose a new rupture model generator in long-period strong ground motion simulations, by improving the Irikura recipe to include the fling step near surface fault ruptures, and apply it to the observation records during the 2016 Kumamoto earthquake. A series of M6-7 earthquakes occurred from April 14 to 16 in 2016 in the Kumamoto prefecture of the Kyushu Island, Japan. The main-shock (Mw7.0, 2016/4/16) generated the extensive surface faulting, and the strong ground motions at Mashiki City and Nishihara Village showed clearly permanent displacements (fling step).

First, we construct a characterized source model (Model-01) in the seismogenic layer for the main shock based on the Irikura recipe. In addition, we expand the Irikura recipe for the shallower region than the seismogenic layer, by evaluating the regularized Yoffe-type slip velocity functions by Tinti et al. (2005). We construct an empirical relation among the fault slip and the parameters of the Yoffe function using the collected source fault models based on the waveform inversion of strong motion data.

Next, we simulate observation records at KiK-net Mashiki and Nishihara Village using the proposed fault models using the theoretical method (Hisada and Bielak (2003)) in the period over 1s. Even though Model-01 reproduced well the record at KiK-net Mashiki, it underestimates the observation waveforms of velocity and displacement at Nishihara Village, which is much closer to surface faulting. One of the reasons for the underestimate is the radiation amplitude patterns of S-waves from the seismogenic layer are small in the near-fault region (<1km). To improve the results, we construct two source models, Model-02 with large slip and short slip duration for the shallower region, and Model-03 including the additional fault model called the Idenoguchi fault located 2km southeast of main fault. The simulated waveforms using these two models showed much better agreement with the observation record. We conclude that Model-03 is more realistic than Model-02, and the geometric shape of the source fault model is important for predicting long-period ground motions including the fling step in the near-fault region.

Finally, we simulated the broadband strong ground motions at KiK-net Mashiki and Nishihara village using Model-03 and the Stochastic Green's Function Method in the short period less than 1s. We confirmed that synthetic waveforms are almost consistent with observed waveforms.

Keywords: Near-fault region，Seismic Waveform Inversion，Fling-Step，Strong ground motion prediction

1. Introduction

A series of M6-7 earthquakes occurred from April 14 to 16 in 2016 in the Kumamoto prefecture of the Kyushu Island, Japan, and caused destructive damage in the local areas[1]. The main-shock (Mw7.0, 2016/4/16) generated the extensive surface faulting. Near-fault strong motions during the earthquake were recorded with high accuracy by the National Research Institute for Earth Science and Disaster Resilience (NIED) strong-motion network (K-NET and KiK-net) and the Japan Meteorological Agency (JMA) and local-government seismic-intensity network. KMMH16 (Mashiki-KiK-net station) and Nishihara Village-Hall station (93048) are located extremely near surface breaks along the Futagawa fault zone. Beside the strong ground motions at KMMH16 and Nishihara Village-Hall station showed clearly permanent displacements (fling step). In the near fault region, it is necessary to evaluate long-period components including the permanent displacement. To generate such long-period components including the permanent displacement near fault region, the shallower region than the seismogenic layer (hereinafter called "SR") must be taken into account. Similar studies have been carried out by several authors (e.g., Irikura et al. (2019) [2]). Therefore, we propose a new procedure for evaluating the parameters of SR using source fault models based on the waveform inversion.
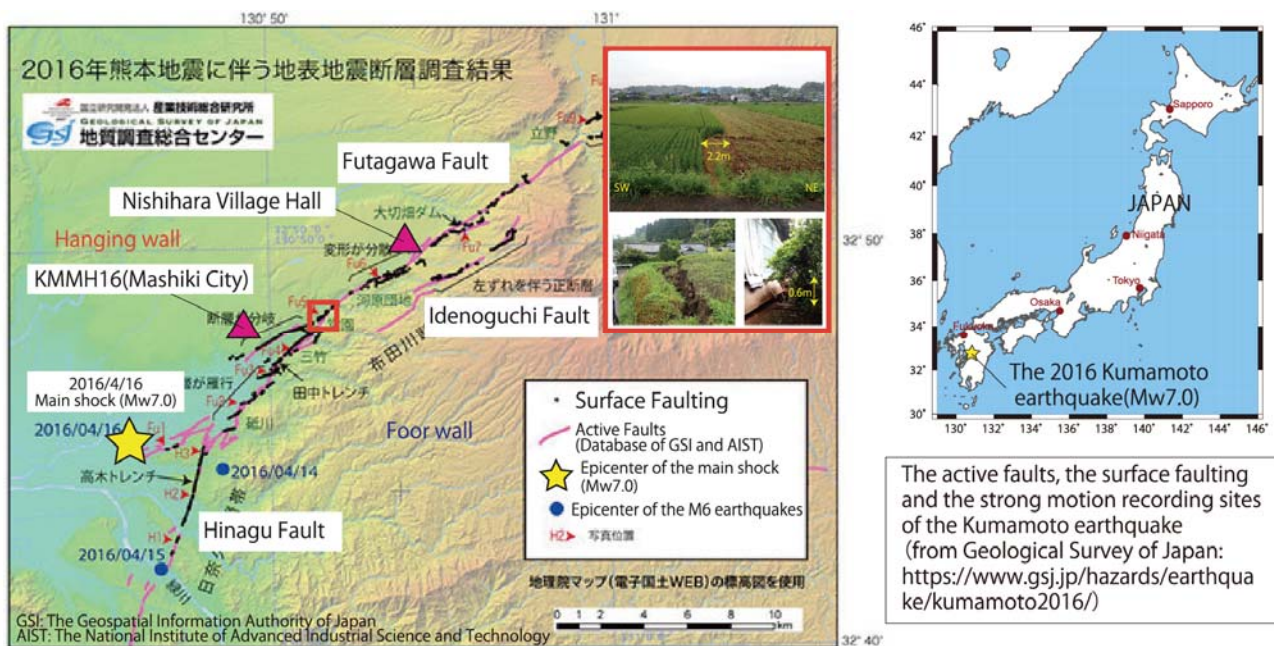
Fig.1 The active faults, the surface faulting and the strong motion recording sites of the 2016 Kumamoto earthquake (from Geological Survey of Japan: https://www.gsj.jp/hazards/earthquake/kumamoto2016/)

2. The slip velocity time function in the shallower region

First, we collected source fault models based on the waveform inversion of strong motion data as shown in Table 1. And we modeled the slip velocity time function in SR by the regularized Yoffe function[3].

Fig.2 and Fig.3 shows the observation records and the synthetic ground motions by the theoretical method for long periods over 1 s at KMMH16 (Mashiki-KiK-net station) for 2016 Kumamoto Earthquake. Ground motions of velocity and displacement of Case1 are simulated using the source fault model based on the source inversion analysis[4] and numerical Green's functions calculated by the wavenumber integration method (Hisada and Bielak (2003) [5]). This method has the particular advantage of being able to simulate ground motions at near-fault stations due to surface faulting with static offset in the formulation because of

2

the removal of near-source singularities by separating the static and dynamic Green's functions. The synthetic motions of Case 1 agree well with the observation records as shown in Fig.3. Case 2 is the evaluation of considering only 10km×4km area in SR near KMMH16. This results stands for the ground motions from the shallower region are dominant for the Fault Parallel component. We then modeled the slip velocity time function of Case2 by the regularized Yoffe function. We set the parameters of the regularized Yoffe function (τ_S and τ_R as shown in Fig.3) it by trial and error to fit the synthetic motions by Case 3 to that by Case 2. In addition, we evaluated other earthquakes and created a regression for relation between slip amount and the parameters of the regularized Yoffe function (τ_S and τ_R) by the results as shown in Fig.4.

Table 1 Collected source fault models based on the waveform inversion of strong motion data

№	Earthquake	Slip model reference	M_W	Observation point[※1]			Frequency(Hz)		Green function[※2]
				SGM	TELE	GPS	Low	High	
1	1992 Landers	Wald and Heaton(1994)[6]	7.3	16	11	42	0.08	0.5	Common
2	1995 Kobe	Wald(1996)[7]	6.9	19	13	20	0.05	0.5	2 types
3	1999 Chi-Chi	Wu et al.(2001)[8]	7.7	47	—	60	0.02	0.5	3 types
4	2002 Denali	Oglesby et al.(2004)[9]	7.9	8	—	38	0.01	0.5	Common
5	2011 Hamadori	Hikima(2012)[10]	6.6	10	—	—	0.05	0.8	Individual
6	2014 Nagano	Hikima et al.(2015)[11]	6.3	12	—	—	0.05	0.8	Individual
7	2016 Kumamoto (main shock)	Hikima(2016)[4]	7.0	18	—	—	0.05	0.8	Individual

※1 : Number of observation points used for analysis . SGM: Strong ground motion stations, TELE : Teleseismic stations, GPS : GPS stations.
※2 : Geotechnical model used for analysis. Common : Common soil profile for all stations, 2 types,3 types : 2 types or 3types of soil profile.
　　　Individual : Different soil profile for each station.
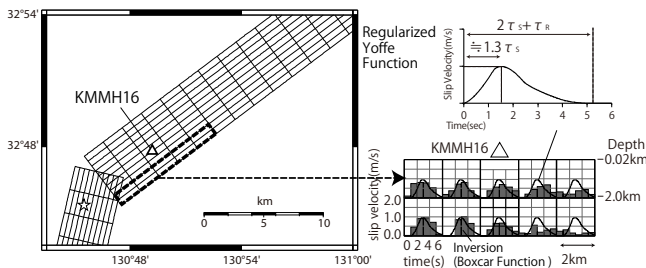
Fig.2 Modeling for slip velocity function by the Yoffe-type slip velocity functions modified by Tinti et al. (2005)
(Example of 2016 Kumamoto earthquake)
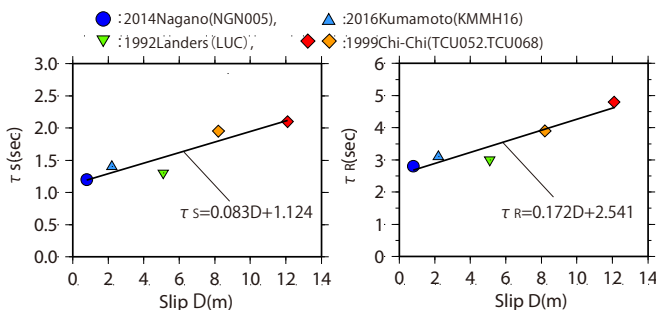
Fig.4 Relation between the slip and the parameters of the Yoffe-type slip velocity functions modified by Tinti et al. (2005)
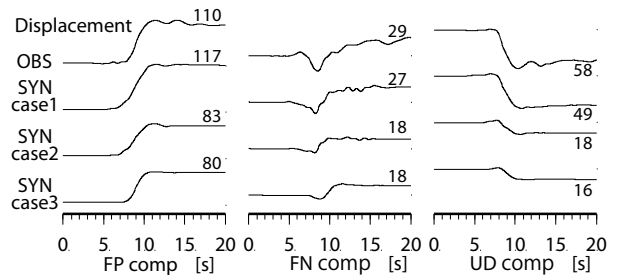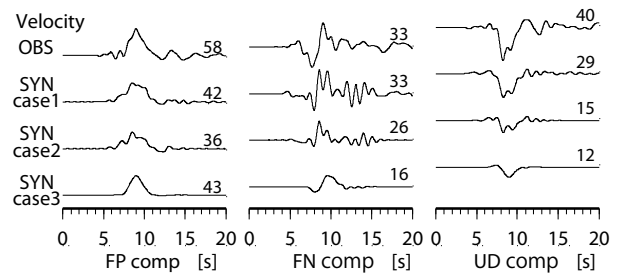
Fig.3 Observed and Synthetic over 1-s low-pass filtered velocity and displacement waveforms at KMMH16 (Maximum amplitude is shown above each waveform in cm/s for velocity and cm for displacement)

Similarly, we compared the slip and length of asperities in seismogenic layer with one in SR as shown in Table 2. We identified shallow asperities and deep asperities based on Somerville et al. (1999) [12] and Kagawa et al. (2005) [13]. We identified asperities from the slip distribution in SR and then we identified deeper asperities from the remaining portion of the fault. The slip and the length of the asperities in seismogenic layer are as much as one in the shallower region than the seismogenic layer. This relationships roughly coincides with the relationships between maximum displacement of the surface rupture and maximum slip of the subsurface seismic fault by Matsushima et al. (2010) [14].

Table 2 Area and slip of individual asperity

№	Earthquake	Name	Area				L (km)	W (km)	D (m)	Continuity	L_{sum} (km)	D_{ave} (m)	Ratio(s/d)	
			X1 (km)	X2 (km)	Y1 (km)	Y2 (km)							L_{sum}	D
1	1992 Landers	s1	9.0	27.0	0.0	2.5	18.0	2.5	5.07	○	36	4.43	1.50	0.88
		s2	30.0	48.0	0.0	2.5	18.0	2.5	3.80	○				
		d1	15.0	21.0	2.5	7.5	6.0	5.0	5.05	○	24	5.06		
		d2	24.0	36.0	2.5	15.0	12.0	12.5	5.25	○				
		d3	45.0	51.0	2.5	15.0	6.0	12.5	4.69	○				
2	1995 Kobe	s1	0.0	19.98	0.0	2.5	19.98	2.5	2.18	○	20	2.18	1.50	1.90
		d1	6.66	19.98	2.5	20.0	13.32	17.5	1.15	○	13.3	1.15		
3	1999 Chi-Chi	s1	6.0	12.0	0.0	6.0	6.0	6.0	5.44	○	58	8.09	0.91	1.15
		s2	24.0	38.0	2.0	6.0	14.0	4.0	6.42	○				
		s3	40.0	50.0	0.0	6.0	10.0	6.0	6.31	○				
		s4	54.0	70.0	0.0	6.0	16.0	6.0	10.01	○				
		s5	70.0	82.0	0.0	6.0	12.0	6.0	9.63	○				
		d1	6.0	30.0	6.0	12.0	24.0	6.0	5.84	○	64	7.01		
		d2	32.0	64.0	6.0	18.0	32.0	12.0	7.47	○				
		d3	50.0	66.0	20.0	32.0	16.0	12.0	7.06	×				
		d4	70.0	78.0	6.0	8.0	8.0	2.0	6.63	○				
4	2002 Denali	s1	50.35	78.35	0	3.75	28.0	3.75	4.88	○(1)	28(1) 48(2)	4.88(1) 4.67(2)	0.58 0.92	0.87 0.72
		s2	138.35	162.35	0	3.75	24.0	3.75	4.39	○(2)				
		s3	166.35	190.35	0	3.75	24.0	3.75	4.95	○(2)				
		d1	30.8	78.8	3.75	15.0	48.0	11.25	5.64	○(1)	48(1) 52(2)	5.64(1) 6.52(2)		
		d2	90.35	114.35	11.25	22.5	24.0	11.25	4.80	×				
		d3	134.35	186.35	3.75	18.75	52.0	15.0	6.52	○(2)				
		d4	190.35	206.35	3.75	11.25	16.0	7.5	5.13	×				
		d5	214.35	226.35	3.75	11.25	12.0	7.5	4.19	×				
5	2011 Hamadori	s1	4.0	20.0	0.0	2.0	16.0	2.0	1.51	○	16	1.51	1.14	1.09
		d1	4.0	18.0	2.0	6.0	14.0	4.0	1.38	○	14	1.38		
		d2	26.0	34.0	2.0	10.0	8.0	8.0	0.86	×				
6	2014 Nagano	s1	4.5	7.5	0.0	3.0	3.0	3.0	0.77	×	—	—	—	—
		d1	7.5	15.0	4.5	10.5	7.5	6.0	0.63	×	—	—		
7	2016 Kumamoto (main shock)	s1	12.0	18.0	0.0	4.0	6.0	4.0	2.76	○	12	2.66	0.75	1.00
		s2	22.0	28.0	0.0	4.0	6.0	4.0	2.57	○				
		d1	12.0	28.0	4.0	14.0	16.0	10.0	2.65	○	16	2.65		
The mean value and the standard deviation (+1 sigma)													1.00 (1.41)	1.04 (1.42)

※s1, d1 : s means the region shallower than the seismogenic layer, d means the seismogenic layer.
　X1, X2,Y1,Y2 : Position of the corner of the asperity, L : Length of asperity ,W : Width of asperity , D : slip of asperity.
　L_{sum} : Total length of asperity(only continuous with the region shallower than the seismogenic layer and the seismogenic layer)
　D_{ave} : Average value of slip in the asperity(only continuous with the region shallower than the seismogenic layer and the seismogenic layer)
　Ratio : The ratio of the region shallower than the seismogenic layer to the seismogenic layer.
　Continuity : If the asperity located in the region shallower than the seismogenic layer
　　　　and the asperity located in the seismogenic layer are in contact, ○.

4

3. Simulation of Near-Fault Ground Motions Using Characterized Source Model

Next, we constructed characterized source model for the Kumamoto earthquake and calculated ground motions by the theoretical method. Parameters in the seismogenic layer are set by the strong ground motion prediction method by the Headquarters for Earthquake Research Promotion[15] (hereinafter called "Recipe"). The slip in the shallower region is the same as that in the seismogenic layer, and the slip velocity time function is the regularized Yoffe function based on the above mentioned results.

3.1 Extension of Characterized Source Model based on the "Recipe"

We construct a characterized source model (Model-01) for the 2016 Kumamoto earthquake based on Recipe. We set two segment fault model with two asperities (one in each segment), based on the inversion result obtained by Hikima (2016)[4]. The depth of the seismogenic layer are 3-19km. The slip velocity time function in the seismogenic layer is a Kostrov-like function developed by Nakamura and Miyatake (2000)[16].

Besides, we construct the characterized source model to extend the Recipe for SR based on this study. We set asperity with large slip in SR above the asperity in the seismogenic layer if assume the surface fault as shown in Fig.5. The slip velocity time function in SR is the regularized Yoffe-type slip velocity functions. The parameters of the regularized Yoffe-type slip velocity functions, τ_S and τ_R are 1.4s and 3.1s based on this study. The source parameters of Model-01 are presented in Table 3.

Table 3 Source parameters of constructed characterized source model

	Parameters	Model-01 (Basic model)	Model-02	Model-03
the Seismogenic Layer	Size (Length×Width)	32km×20km(Futagawa) 12km×20km(Hinagu)		Same as the left column and 13km×10km(Idenoguchi)
	Strike	233°(Futagawa), 193°(Hinagu)		Same as the left column and 231°(Idenoguchi)
	Dip	75°(Futagawa), 78°(Hinagu)		Same as the left column and 65°(Idenoguchi)
	Rake	-160°		Same as the left column and -110°(Idenoguchi)
	Moment	$3.1×10^{19}$Nm		$4.0×10^{19}$Nm
Shallower Region than the Seismogenic Layer	Slip	Recipe×1.0	Recipe×1.4(asperity)	Recipe×1.0
	Rake	-160°	-135°	-160°
	Slip velocity function	the regularized Yoffe τ_S=1.4s, τ_R=3.1s	the regularized Yoffe τ_S=0.7s, τ_R=1.6s	the regularized Yoffe τ_S=1.4s, τ_R=3.1s
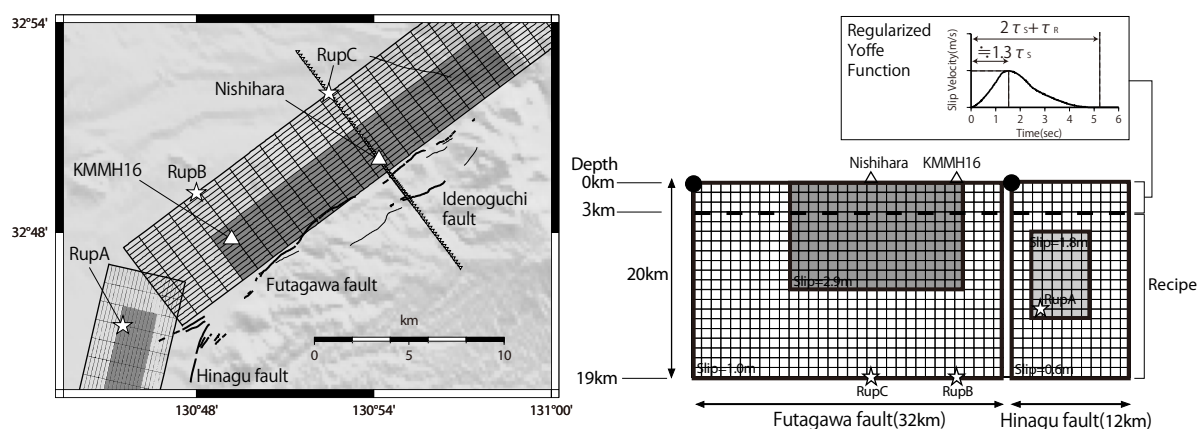
Fig.5 Characterized source model (Model-01) with elevation[19], rupture starting point (☆), active faults[20] (bold line: active fault trace, thin line: active faults estimated), strong motion stations (△), and points orthogonal to Futagawa fault through Nishihara Village-Hall station (▽)

5

We simulate observation records at KMMH16 (Mashiki-KiK-net station) and Nishihara Village-Hall station using this source fault models by the theoretical method in the period over 1s. KMMH16 is located about about 2.1 km away from surface traces along the Futagawa fault and Nishihara Village-Hall station is located about 0.8 km away from surface traces along the Futagawa fault. Ground motions of velocity and displacement are simulated using Model-01 and numerical Green's functions calculated by the wavenumber integration method (Hisada and Bielak (2003)). We use a one-dimensional velocity structure model by J-SHIS[17] for each station. The extreme pulse-like waveforms observed at these near-fault stations can be attributed to the event's upward rupture[18]. The starting points in Model-01 are hypocenter for 2016 Kumamoto Earthquake(RupA as shown in Fig.5) and below each stations(RupB and RupC as shown in Fig.5).

Fig.6 shows the comparison of the observation records and the synthetic ground motions. The synthetic ground motions agree well with the observation records at KMMH16. On the other hand, synthetic velocity motions at Nishihara Village-Hall station obtained using Model-01 are clearly underestimated compared with the observed ones, as shown in Fig. 6. Despite Nishihara Village-Hall station is located at the very near-fault, synthetic velocity motions from the seismogenic layer (orange line in Fig.6) in Nishihara Village-Hall station is smaller than one in the KMMH16.

(1) over 1-s low-pass filtered velocity

(2) over 1-s low-pass filtered displacement
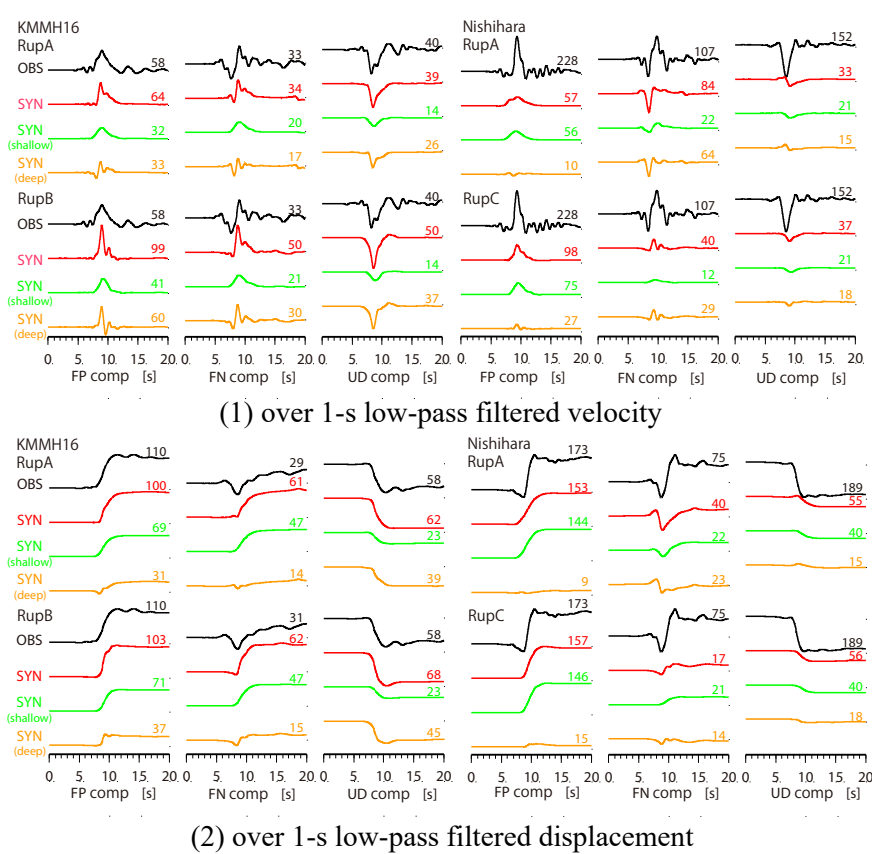
Fig.6 Observed and synthetic waveforms for Model-01 (Maximum amplitude is shown above each waveform in cm/s for velocity and cm for displacement)
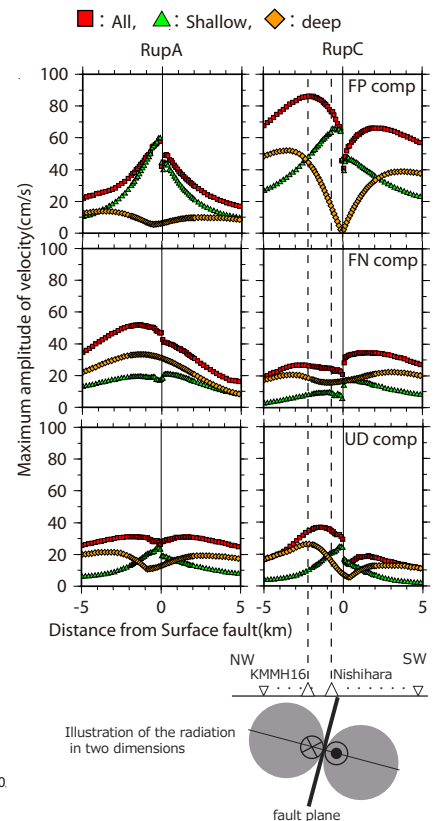
Fig.7 The distribution of maximum amplitude of velocity at points orthogonal to Futagawa fault through Nishihara Village

6

One of the differences between KMMH16 and Nishihara Village-Hall station is the distance from the surface fault. Thus we calculated the ground motions at virtual points orthogonal to Futagawa fault through Nishihara Village-Hall station as shown in Fig.5. We assume the homogeneous half-space in this calculation. Fig.7 shows distribution of maximum velocity at virtual points orthogonal to Futagawa fault through Nishihara Village-Hall station. The more distance from fault trace is near, synthetic velocity motions from SR is large. On the other hand, synthetic velocity motions from the seismogenic layer within 1 km from surface fault are clearly smaller. The radiation amplitude patterns of S-waves from the seismogenic layer are small within 1 km from surface fault. That is one of the reasons for the underestimate.

Therefore, there are two ways to modify the source model. One is to modify the parameters of the shallower region because the contribution is large. It is necessary to increase the amount of slip and shorter the slip velocity time function. The other is to modify the geometric shape of source model. There are Idenoguchi fault that is located about 2 km from Nishihara Village-Hall station where ground motions from the seismogenic layer becomes large by directivity effects.

3.2 Modification of Characterized Source Model

We construct two modified source models as shown in Fig.8. Model-02 with large slip and short slip duration (τ_S and τ_R are 0.7s and 1.6s) for shallower region than the seismogenic layer and Model-03 with the additional fault plane. The additional fault plane in Model-03 is Idenoguchi fault with large rupture velocity. The source parameters of Model-02 and Model-03 are presented in Table 3.

Fig.9 shows the strong ground motion records and calculated motions using the modified models by the theoretical method for long periods over 1 s. By and large, synthetic waveforms produced with these two models waveforms are in much closer agreement with observed waveforms.
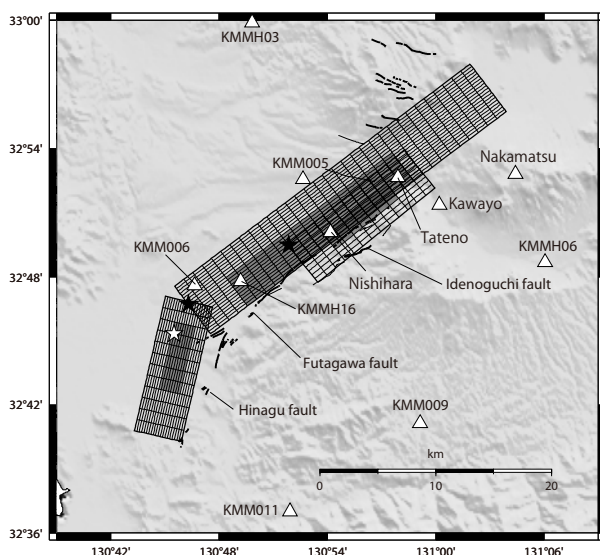
(1) Location of characterized source model（Model-03）
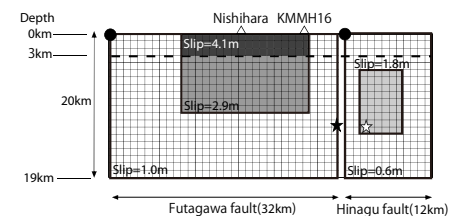
(2) Slip distributions for Model-02
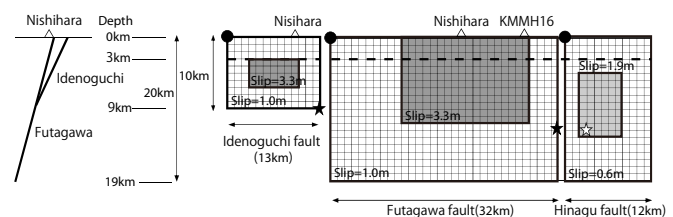
(3) Slip distributions for Model-03

Fig.8 Characterized source model (Model-02 and Model-03) with elevation[19], active faults[20] (bold lines: active fault traces, thin lines: estimated active faults), triangles: strong motion stations

7
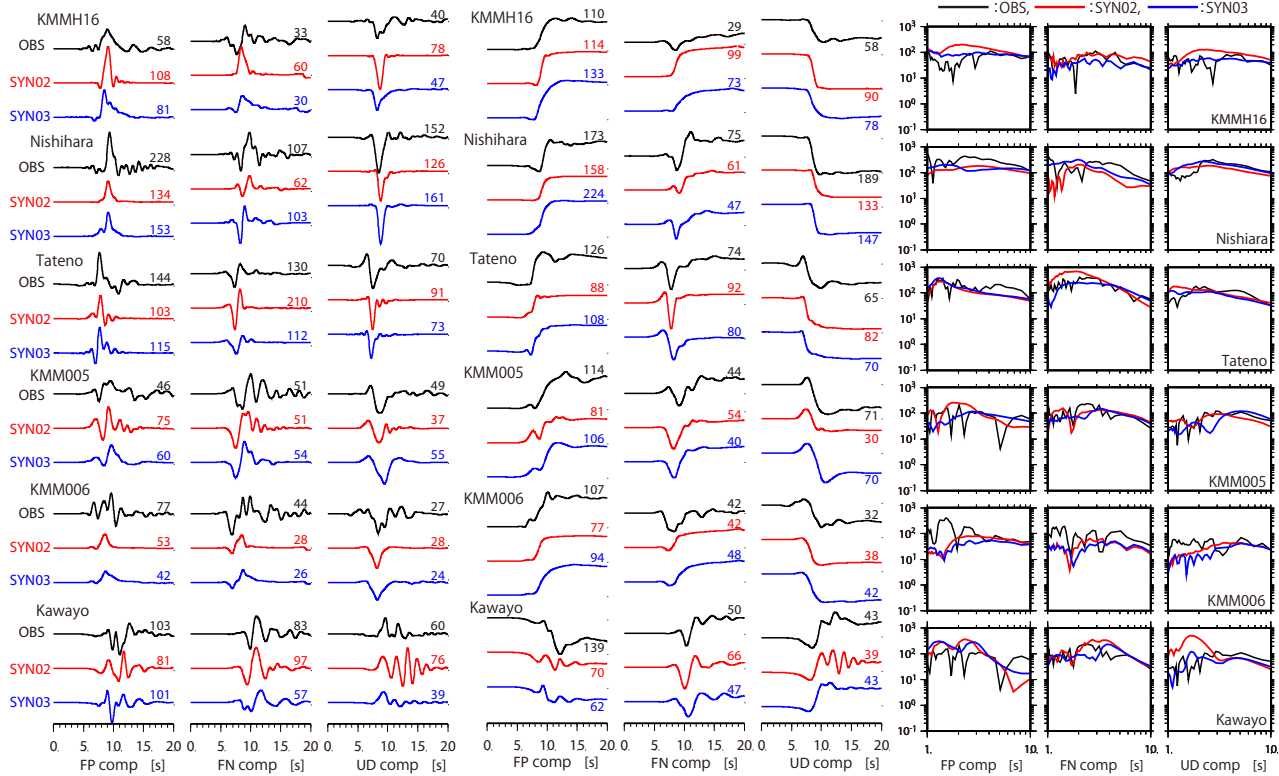
(a) over 1-s low-pass filtered velocity (b) over 1-s low-pass filtered displacement (c) Acceleration Fourier spectra
(1) Six stations near Futagawa fault
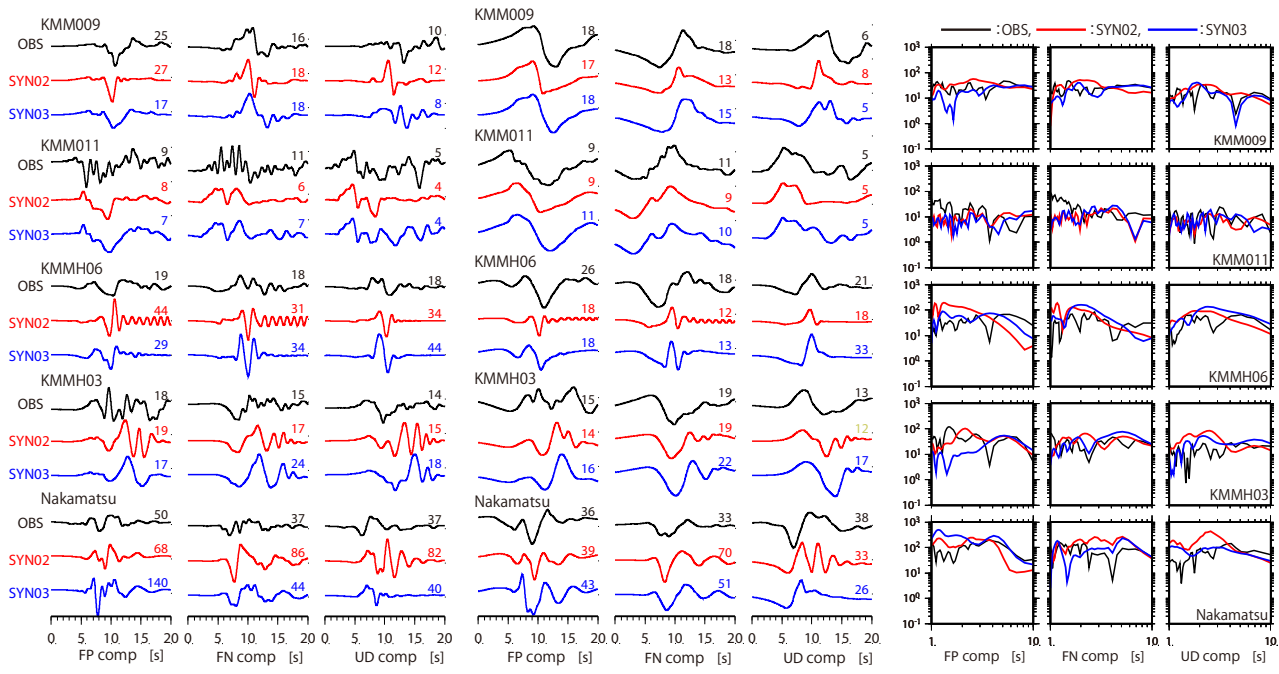
(d) 1 to 20 s band-pass filtered velocity (e) 1 to 20 s band-pass filtered displacement (f) Acceleration Fourier spectra
(2) Five stations slightly further away from Futagawa fault

Fig.9 Observed and Synthetic waveforms and acceleration Fourier spectra for Model-02(SYN02) and Model-03(SYN03) (Maximum amplitude is shown above each waveform in cm/s for velocity and cm for displacement)

8

(1) Model-02

(2) Model-03
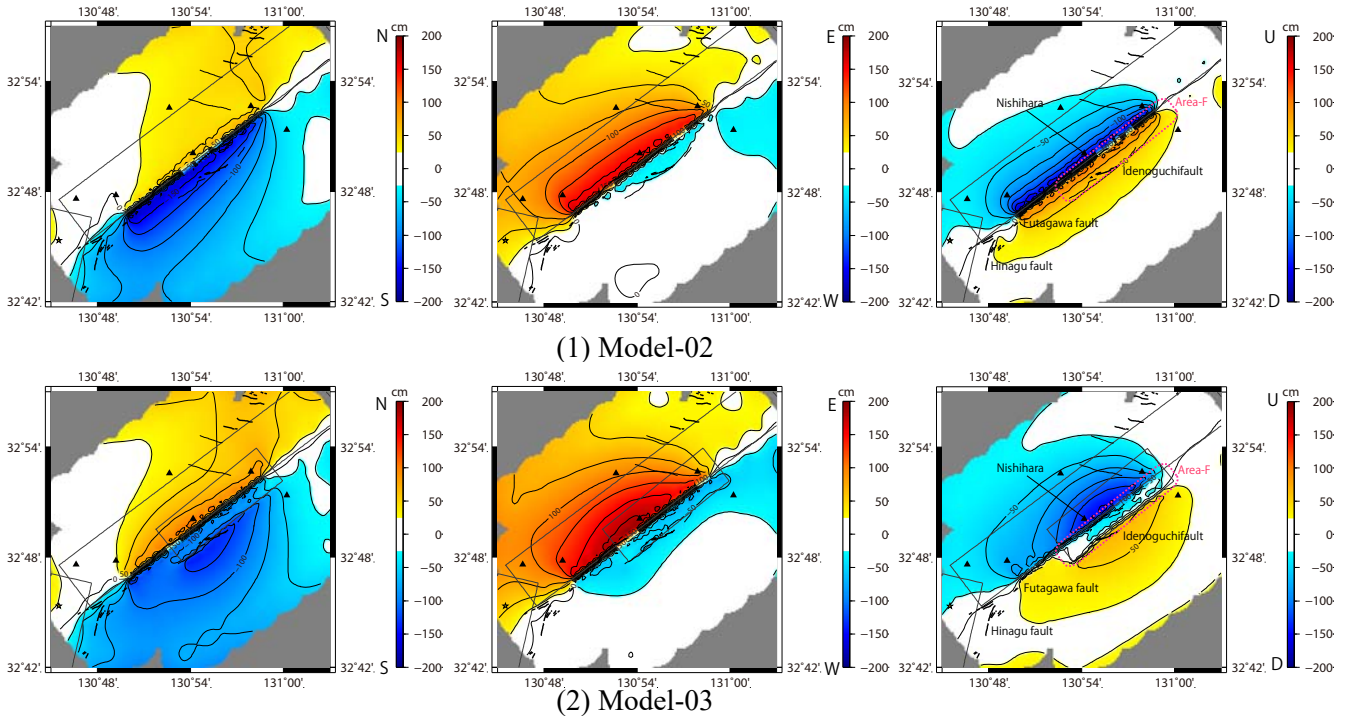
Fig.10 Synthetic permanent displacement distributions (NS component(left), EW component (center), UD component (right))
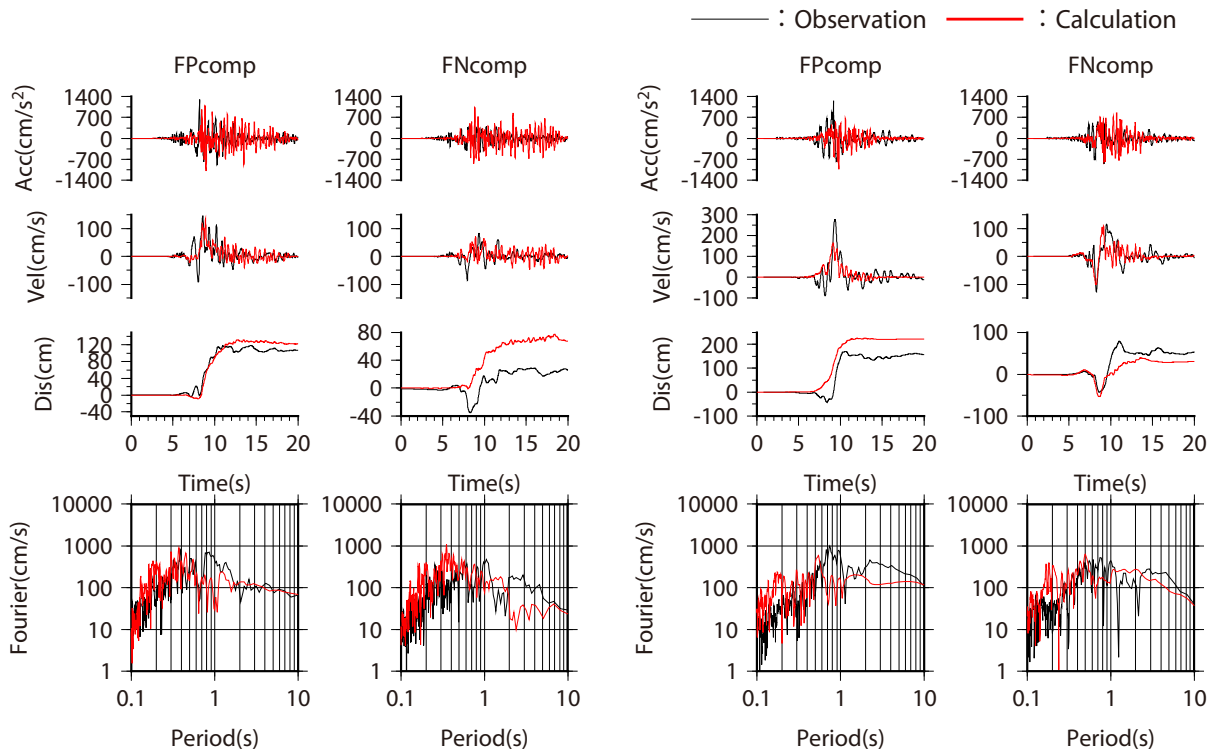
(1) KMMH16 (Mashiki-KiK-net station, Surface)　　　(2) Nishihara Village-Hall station

Fig.11 Observed and Synthetic (Hybrid method) waveforms and acceleration Fourier spectra for Model-03(SYN03)

9

On the other hand, the slip on the asperity for SR (=4.1m) of Model-02 is larger than the maximum slip of surface ruptures (=2.2m) based on the survey by Shirahama et al. (2016)[21]. Fig.10 shows the synthetic permanent displacement distributions. Here we focused on the region between Futagawa fault and Idenoguchi fault. The displacement in the region between Futagawa fault and Idenoguchi fault calculated by Model-02 is uplift. In contrast, the displacement based on ALOS-2/PALSAR-2 by Himematsu and Furuya (2016) [22] is sedimentation in the region. These are a significant difference. Considering these results, we conclude that the Model-03 can describe the actual phenomenon best. This result suggests that geometric shape of the source fault model is important for predicting long-period ground motions containing permanent displacement in the near-fault region.

Finally, we simulated the broadband strong ground motions at KMMH16 (Mashiki-KiK-net station) and Nishihara Village-Hall station using Model-03 and the Stochastic Green's Function Method in the short period less than 1 s. We use a one-dimensional velocity structure model by J-SHIS[17] with $Q=100f^{1.0}$ in Nishihara Village-Hall station. On the other hand, we use a one-dimensional velocity structure model by Tanaka et al.(2019) [23] for shallower than G.L.-252m and J-SHIS[16] with $Q=100f^{1.0}$ for deeper than G.L.-252m in KMMH16. We confirmed that synthetic waveforms are almost consistent with observed waveforms as shown in Fig.11.

4. Conclusions

We proposed a new procedure for evaluating the parameters of characterized fault model for predicting long-period ground motions containing permanent displacement in the near-fault region. First, we collected source fault models based on the waveform inversion of strong motion data. The slip velocity function in the region shallower than seismogenic layer is approximated as the regularized Yoffe-type slip velocity functions by Tinti et al. (2005). We evaluated the relation of the slip and the parameters of the regularized Yoffe function.

Next, we constructed characterized source models for the 2016 Kumamoto earthquake by the new procedure that based on strong ground motion prediction method by the Headquarters for Earthquake Research Promotion ("Recipe"). Besides, we expanded the Recipe based on the above mentioned results for shallower region than the seismogenic layer. We recommended the regularized Yoffe-type slip velocity functions for shallower region than the seismogenic layer.

Finally, we constructed two source models, Model-02 with large slip and short slip duration for shallower region than the seismogenic layer and Model-03 with the additional fault plane. The additional fault plane in Model-03 is Idenoguchi fault with large rupture velocity. By and large, synthetic waveforms produced with these two models waveforms are in much closer agreement with observed waveforms. On the other hand, the displacement in the region between Futagawa fault and Idenoguchi fault calculated by Model-02 is uplift. In contrast, the displacement based on ALOS-2/PALSAR-2 by Himematsu and Furuya (2016) [22] is sedimentation in the region. These are a significant difference. Considering these results, we concluded that the Model-03 can describe the actual phenomenon best. This result suggests that geometric shape of the source fault model is important for predicting long-period ground motions containing permanent displacement in the near-fault region.

5. Acknowledgements

6. References

[1] Building Research Institute (2016): Building Damage Investigation Report of the 2016 Kumamoto Earthquake (Preliminary Report), NILIM Report, 929 (BRI Report, 173) (in Japanese).

[2] I Irikura, K., Kurahashi, S. & Matsumoto, Y. Pure Appl. Geophys, https://doi.org/10.1007/s00024-019-02283-4, pp. 1-27, 2019. 8

[3] Tinti, E. et al.: A Kinematic Source-Time Function Compatible with Earthquake Dynamics, Bulletin of the Seismological Society of America, Vol. 95, No. 4, pp. 1211-1223, 2005. 8

[4] Hikima, K.: Source rupture process of the 2016 Kumamoto earthquake and its foreshock estimated from strong-motion waveforms, JAEE annual meeting 2016, P 4-11, 2016. 9 (in Japanese)

[5] Hisada, Y., & Bielak, J. (2003). A theoretical method for computing near-fault ground motions in layered half-spaces considering static offset due to surface faulting, with a physical interpretation of fling step and rupture directivity. Bulletin of the Seismological Society of America, 93, 1154–1168.

[6] Wald, D. J., and T. H. Heaton: Spatial and Temporal Distribution of Slip for the 1992 Landers, California, Earthquake, Bulletin of the Seismological Society of America, Vol.84, No.3, pp. 668-691, 1994. 6

[7] Wald, D. J: Slip history of the 1995 Kobe, Japan, earthquake determined from strong motion, teleseismic, and geodetic data, J. Phys. Earth, Vol. 44, No. 5, pp. 489-503, 1996. 1

[8] Wu, C. J. et al.: Source process of the Chi-Chi earthquake: A joint inversion of strong motion data and global positioning system data with a multifault model, Bulletin of the Seismological Society of America, Vol. 91, No. 5, pp. 1128-1143, 2001.10

[9] Oglesby, D. D. et al.: Inverse kinematic and forward dynamic models of the 2002 Denali fault earthquake, Bulletin of the Seismological Society of America, Alaska, Vol. 94, No. 6, pp. 214-233, 2004. 12

[10] Hikima, K.: Rupture Process of the April 11, 2011 Fukushima Hamadori Earth quake(Mj7.0) : Two Fault Planes Inferred from Strong Motion and Relocated Aftershocks , Zishin, Vol. 64, No. 4, pp. 243-256, 2012. 6 (in Japanese)

[11] Hikima, K. et al.: Source process of the 2014 Nagano-Ken Hokubu Earthquake(Mj6.7) 〜Analysis using the near-field Broadband Waveforms in the source region〜 , Fall meeting of 2015 Seismological Society of Japan, S15-14, 2015. 9 (in Japanese)

[12] Somerville, P. G. et al.: Characterizing crustal earthquake slip models for the prediction of strong ground motion, Seismological Research Letters, 70, pp. 59-80, 1999. 1

[13] Kagawa.T. et al.: Differences in ground motion and fault rupture process between the surface and buried rupture earthquakes, Earth Planets Space, 56, pp. 3-14, 2004. 6

[14] Matsushima, S. et al.: Scaling relations of earthquakes on active mega-fault systems, Geophysical Bulletin of Hokkaido University, No. 73, pp. 117-127, 2010. 3 (in Japanese)

[15] Headquarters for Earthquake Research Promotion, "Strong ground motion prediction method ("Recipe") for earthquakes with specified source faults," 2009 (in Japanese).

[16] Nakamura, H., & Miyatake, T. (2000). An approximate expression of slip velocity time functions for simulation of near-field strong ground motions. Zisin, 53, 1–9. (In Japanese with English abstract).

[17] Fujiwara, H. et al.: Some Improvements of Seismic Hazard Assessment based on the 2011 Tohoku Earthquake, Technical Note of the National Research Institute for Earth Science and Disaster Prevention, No. 379, 2012. 12 (in Japanese)

[18] Miyatake, T.: A consideration on the strong fault parallel pulse at Mashiki, Fall meeting of 2016 Seismological Society of Japan, S21-P05, 2016. 10 (in Japanese)

[19] Geographical Survey Institute: Digital map 50m grid (elevation), Japan-III, CD-ROM version, 1997. (in Japanese)

[20] Nakata, T. and T. Imaizumi: Digital active fault map of Japan, University of Tokyo press, 2002. (in Japanese)

[21] Shirahama, Y. et al.: Characteristics of the surface ruptures associated with the 2016 Kumamoto earthquake sequence, central Kyushu, Japan, Earth Planets Space, Vol. 68:191, doi:10.1186/s40623-016-0559-1, 2016. 11

[22] Himematsu, Y. and M. Furuya: Fault source model for the 2016 Kumamoto earthquake sequence based on ALOS-2/PALSAR-2 pixel-offset data: evidence for dynamic slip partitioning, Earth, Planets and Space, Vol. 68:196, doi:10.1186/s40623-016-0545-7, 2016. 10

[23] Tanaka, S. et al.: Relation between Strong Ground Motions and Building Damage in KiK-net Mashiki and the Shimojin Areas during the 2016 Kumamoto Earthquake, Journal of JAEE, Vol.19, No.5, pp. 59-76, 2019. 9 (in Japanese)